

Effect of Cd Addition on Superconducting Fluctuations and Mechanical Properties of $\text{Bi}_{1.82}\text{Pb}_{0.36}\text{Sr}_2\text{Ca}_2\text{Cd}_x\text{Cu}_3\text{O}_y$ System

S. M. Khalil

Physics Department, Faculty of Science, South Valley University, Sohag, Egypt
E-mail: khalil.20002000@yahoo.com

(Received August 31, 2005; revised November 23, 2005)

A study was made of the effect of Cd additions on the superconducting and mechanical properties of $\text{Bi}_{1.82}\text{Pb}_{0.36}\text{Sr}_2\text{Ca}_2\text{Cd}_x\text{Cu}_3\text{O}_y$ ($x = 0.0, 0.15, 0.25, 0.35$ and 0.55). Characterization of the Cd-samples using XRD, DTA, and SEM techniques, has confirmed that remarkably formation of low- T_c phase (2212) by the addition of Cd up to 0.35. High-resolution electrical resistivity $\rho(T)$ data on the composition of Cd=0.35 have been taken for investigating critically the superconducting fluctuations. Using the Aslamazov and Larkin (AL) and Lawrence and Doniach (LD) models of excess conductivity. Excess conductivity analysis shows that this composition (Cd=0.35) is 2D in the temperature range 137.8–163.7 K and a 3D one below 137.8 K. Thus, a crossover from 2D to 3D is observed at 137.8 K. Sample microhardness and density are greatly improved by Cd-additions (0.35). This trend is probably due to the intercalation of cadmium between superconducting grains in compositions may provide a plastic-flow region that allows relaxation of undesirable stresses resulting from the grain anisotropy of superconductors.

KEY WORDS: $\text{Bi}_{1.82}\text{Pb}_{0.36}\text{Sr}_2\text{Ca}_2\text{Cd}_x\text{Cu}_3\text{O}_y$ compound; addition; excess Conductivity; DTA; high- T_c phase (2223); low- T_c phase (2212); microhardness; porosity.

1. INTRODUCTION

It has been well established that, in the Bi–Sr–Ca–Cu–O system of high- T_c oxides superconductors, there are three phases responsible for transition temperatures (T_c°), i.e. 110 K (2223) phase, 85 K (2212) phase and 20 K (2201). Dopant as one of the important method often used during the ceramic processing to modify the characteristics of the material produced. However, several successful attempts have been directed

towards obtaining a best superconducting results by incorporating suitable amount of lead into bismuth system.^{1,2} An interesting results has been reported on the influence of addition of Cd in raising T_c^o from 80 to 100 K in Bi-system.³⁻⁵ The increase of T_c^o has also been reported in Cd-doped (Pb,Cu)Sr₂(Y,Ca)Cu₂O_{7- δ} ,^{6,7} the highest T_c (onset) is up to 92 K in this system, Cd²⁺ ions mainly substitute within the rock-salt-type layer incorporating Pb⁴⁺. Also, the authors^{8,9} have successfully synthesized Bi-1212 superconducting cupartes with a (Bi,Cd)O monolayer. In this circumstance it is of interest to investigate the effects of the Cd-addition on the superconducting fluctuations and mechanical parameters of the ceramic samples of Bi_{1.82}Pb_{0.36}Sr₂Ca₂Cd_xCu₃O_y (0.0 \leq x \leq 0.55). The best results have been reported for sample of Cd = 0.35. The salient features of this composition, besides their high transition temperature, are the quasi-2D character and short coherence length. The study of excess conductivity provides useful information about some of the fundamental aspects including the mechanism of superconductivity. There have been studies on the excess conductivity along the lines of the Aslamazov and Larkin (AL) and Lawrence and Doniach (LD) models. These investigations have been carried out on samples of either mixed phases (80 and 110 K) or with a long tail of low- T_c phase in the $\rho(T)$ diagram.¹⁰ It is worthmentioning here that T_c^o is very much sensitive to the sample inhomogeneities which ultimately tend to broaden the transition width (ΔT_c). Also, Mandal et al.¹¹ have observed a distinct 2D-3D crossover in excess conductivity behaviour for Bi₂Sr₂Ca₁Cu₂O_x near T_c^o .

On the other hand, mechanical properties of high temperature ceramic superconductors (HTCS) may be the most important consideration, aside of critical current density, in most practical applications. High- T_c superconductors have relatively poor mechanical properties (elastic modulus, fracture toughness and hardness), which limits the use of these materials in practical applications. One of the important strategies to improve these mechanical properties was the doping process. For BSCCO, modification of the mechanical properties can be achieved by Y³⁺ addition,¹² Khalil proved that Y-addition (0.35) improves the mechanical connections between grains consequently the mechanical resistance is increased. Additions of Ba²⁺ has also shown improvement in fracture toughness of bulk BSCCO and the same time enhancing the superconducting properties.¹³ A 45% addition to bulk BSCCO resulted in toughness increase from 6.27×10^{-3} to 13×10^{-3} MPa \sqrt{m} .¹³ Another approach to improve the mechanical properties of BSCCO superconductors is development of microstructure.¹⁴ Based on the beneficial effect of Cd addition to BSCCO, the objective of this study was to perform a detailed evolution of the

effects of Cd additions on the mechanical and superconducting properties of BSCCO superconductors, relating to the change of microstructure.

2. MATERIALS AND EXPERIMENTAL TECHNIQUES

The investigated samples of the nominal composition of $\text{Bi}_{1.82}\text{Pb}_{0.36}\text{Sr}_2\text{Ca}_2\text{Cd}_x\text{Cu}_3\text{O}_y$ ($x = 0.0, 0.15, 0.25, 0.35,$ and 0.55) were prepared by the standard solid state reaction technique. High grade (99.999%) oxides and carbonates powders were well mixed and ground in an agate mortar, the mixture was pre-heated at 800°C in air for 20 h. The resulting powders were ground again and pressed into disk shape pellets by applying a load of 49 KN. After cold pressing, the pellets were sintered at $870\text{--}890^\circ\text{C}$ for 60 h in air. After sintering, the samples were furnace-cooled. The electrical property of the samples was carried out by ordinary four probe method at temperature range $77\text{--}300\text{ K}$. Conductive silver paint was used for contacts. A copper-constantan thermocouple was employed to measure the sample temperature. To characterize the mechanical properties of the synthesized materials the microhardness was investigated on E. Ltd. Wetzlar microhardness tester. Each indentation was separated from previous or specimen edge by at least twice (usually five times) its anticipated length. Loads applied were (0.25, 0.49 and 0.98 N). The diamond indenter had a descent time adjusted to 28 s, the maximum allowed, its dwell time, during when static or quasi-static loading took place, lasted 15 s. Care was taken in cleaning its tip with acetone between each loading.

The Vickers hardness (VHN) was determined using the following formula:

$$VHN = 1.8544 (P/d^2),$$

where “P” is the applied load in N and “d” is the diagonal length of indenter impression in (m.m).

In most materials, the elastic modulus E is related to the bulk hardness H_v by the relation $E = 81.9635 H_v$ [14].

The structural evolution of Cd-samples was performed by using a Schemdzu X-ray powder diffractometer (XRPD) with $\text{CuK}\alpha$ radiation and a constant scan rate of $2\Theta = 4\text{--}50^\circ$. On the other hand, the microstructural investigations were performed using a Jeol JSM-5300 scanning electron microscope (SEM). The melting behaviour of the examined samples was analyzed by differential thermal analysis (DTA). DTA investigations were performed using a Schimadzu differential thermal analysis-50. The rate of heating equal to $10^\circ\text{C min}^{-1}$. Relative density and porosity were performed by Archimedes method.

3. RESULTS AND DISCUSSION

3.1. X-ray Diffraction Investigation

Figure 1(a–c) shows the sequence of X-ray diffraction patterns of the Cd-addition samples of $\text{Bi}_{1.82}\text{Pb}_{0.36}\text{Sr}_2\text{Ca}_2\text{Cd}_x\text{Cu}_3\text{O}_y$ ($0.0 \leq x \leq 0.35$). Open circles, crosses and closed triangles in this figure indicate the high- T_c (2223), low- T_c phase (2212) and 2234 phase. Figure 1(a) shows that the sample of free Cd ($x=0.0$), contains mainly low- T_c phase (2212), the high- T_c phase (2223) and the 2234 phase are also still clear. The last one phase having T_c^0 of 95 K was reported by W. Xiaolin et al.¹⁵ Figure 1(b) shows raise in the low- T_c phase (2212) and decrease in the superconducting phases (2223 and 2234) in sample with enrich in Cd content ($x = 0.25$). It is worth mentioning that, the sample of 0.25 contains superconducting phases (2223 and 2234) but the superconducting transition steps of these two phases have not been detected in the resistivity–temperature

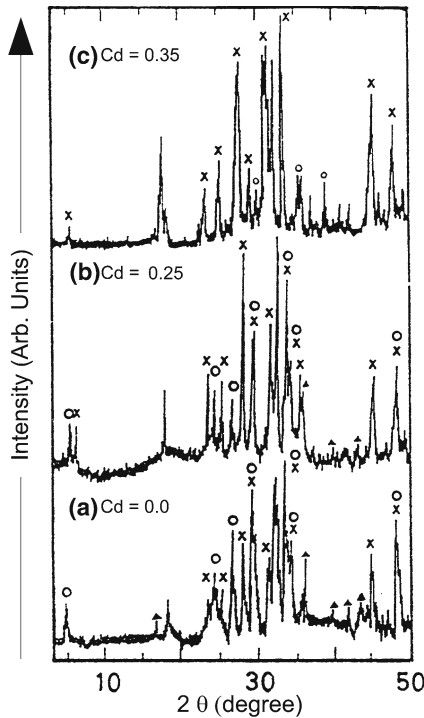


Fig. 1. (a–c) X-ray powder diffraction data for $\text{Bi}_{1.82}\text{Pb}_{0.36}\text{Sr}_2\text{Ca}_2\text{Cd}_x\text{Cu}_3\text{O}_y$, $x = 0.0, 0.25$ and 0.35 . Open circles (High- T_c phase), Crosses (Low- T_c phase), Closed triangles (2234 phase).

measurement, see Fig. 3, this is due to the less content of 2223 and 2234 phase than that 2212 phase or a lack of connectivity between the grains containing these two phases. In Fig. 1(c), the sample of $x = 0.35$ seems completely domination of low- T_c phase (2212) and nearly disappearance of superconducting phases (2223 and 2234). This behaviour may be due to the transformation of 2223 and 2234 into 2212 phase by cadmium doping. From the above results of X-ray diffraction, it can be suggested that the amount of $\text{Cd} = 0.35$ is quite effective in domination of low- T_c phase (2212). However, these results are agree with the authors.^{15,16}

3.2. Differential Thermal Analysis (DTA) Results

In order to investigate the role of Cd element on the formation of 2212 phase together with the disappearance of 2223 phase and 2234 phase in the system of $\text{Bi}_{1.82}\text{Pb}_{0.36}\text{Sr}_2\text{Ca}_2\text{Cd}_x\text{Cu}_3\text{O}_y$ ($0.0 \leq x \leq 0.55$), DTA was performed. Figure 2(a-d) shows the DTA pattern of Cd-samples ($x = 0.0, 0.15, 0.25$ and 0.35) respectively. This figure indicates that a decrease in melting temperature T_m of the Cd-doped samples with increasing in Cd content from 882°C for $x = 0.0$ to 860°C for $x = 0.35$. This reduction in

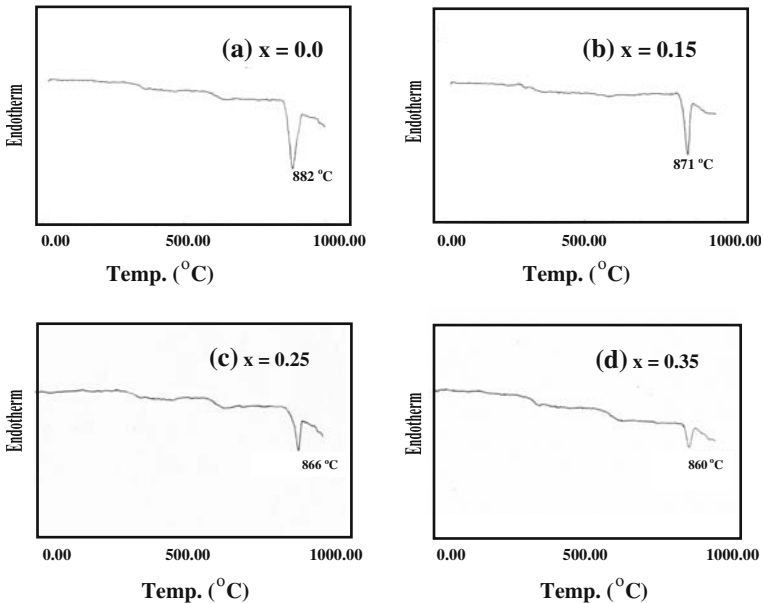


Fig. 2. (a-d) DTA curves of the powders for the system of $\text{Bi}_{1.82}\text{Pb}_{0.36}\text{Sr}_2\text{Ca}_2\text{Cd}_x\text{Cu}_3\text{O}_y$, (a) $\text{Cd}(x = 0.0)$, (b) $\text{Cd}(x = 0.15)$, (c) $\text{Cd}(x = 0.25)$, (d) $\text{Cd}(x = 0.35)$.

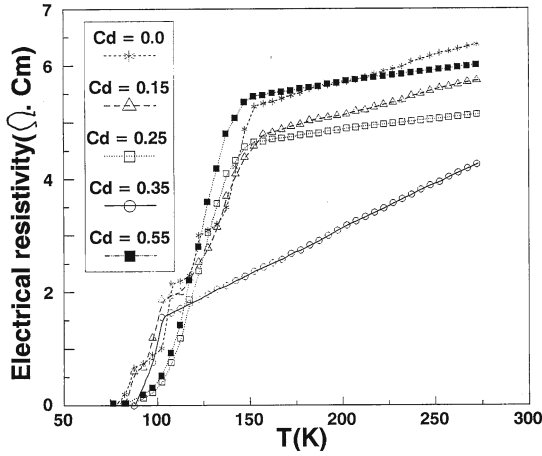


Fig. 3. Electrical resistivity versus temperature of $\text{Bi}_{1.82}\text{Pb}_{0.36}\text{Sr}_2\text{Ca}_2\text{Cd}_x\text{Cu}_3\text{O}_y$ ($x = 0.0 - 0.55$).

melting temperature may be attributed to the addition of Cd lowered the optimum temperature for the mixture, which facilitates the growth of 2212 phase. Such observed reduction in T_m emphasizes the role of Cd-addition on the internal structure of the examined samples. This result was recommended by S. Bernik et al.,¹⁷ they claimed that the 2223 phase melts above 860°C and decomposes into 2212 phase. Besides, Honda et al.¹⁸ suggested that the substitution of K into Ca site lowered the melting point of mixture and the high- T_c phase cannot be formed. The disappearance of the 2223 phase and the 2234 phase by the addition of Cd element to the Bi-system also means the crystal structure of 2212 phase is more stable than that of 2223 and 2234 phase by the substitution of Cd element.

3.3. Electrical Properties

The electrical properties of the samples were examined by resistivity versus temperature measurements ($\rho-T$). Figure(3) plots the variation in sample resistivity with temperature for Cd-doped samples $\text{Bi}_{1.82}\text{Pb}_{0.36}\text{Sr}_2\text{Ca}_2\text{Cd}_x\text{Cu}_3\text{O}_y$ ($0.0 \leq x \leq 0.55$). For all samples, as the temperature is lowered, the initial decrease in resistivity is almost linear. This variation is characteristic of a metal having ohmic behaviour. In Fig. 3, the as-sintered sample seems a metal and turned to complete superconductor through three stages around 123, 108 and 85 K, respectively. After that sequence and gradually decrease in resistivity to zero at $T_c^0 \approx 77$ K. These anomalous resistivity drops can be attributed to the competition between multiphases in this

compound and these phases may have different T_c^0 . Addition of Cd = 0.15 to the parent sample reduces these three stages to two stages around 101 and 88 K, respectively which was followed by a fall in electrical resistivity to reach zero value at $T_c^0 \approx 83$ K. A significantly different temperature dependence of resistivity is observed in the sample of $x = 0.25$, only one superconducting transition takes place around $T^{\text{ons}} \approx 121$ K. Thereafter, the electrical resistivity falls off relatively slowly, and it drops to zero at $T_c^0 \approx 86$ K. For the sample of $x = 0.35$, it can be noticed that the sample behaves the same behaviour of the above sample but it is distinguished with a drastic drop in the resistivity in the form of a very sharp and single transition and ultimately the resistivity becomes zero at $T_c^0 \approx 88$ K. This behaviour is ascribed to the swallow of the metastable phases within the stable superconducting phase, i.e. the sample contains nearly only 2212 phase. However, these results are confirmed by X-ray analysis. Whereas, for higher Cd contents ($x = 0.55$), T_c^0 slightly decreased (~ 84 K). This decrease is due to the addition of Cd acting as a non-bonded solute and causing the weakening of the correlation between the Cu–O layers separated by Cd, thus leading to the depression of T_c^0 .¹⁹ Also, this decrease of T_c^0 may be related to intergrowth of non-superconducting phases. Thereby this intergrowth reduces the superconducting path through grains.¹ On the other hand, it can be observed that an interesting result, the room temperature resistivity of the Cd-doped samples decreased to a minimum value with increasing the doping of Cd from $x = 0.0$ to 0.35, thereafter it increased again. This behaviour can be attributed to the reduction in resistivity with increasing Cd content up to 0.35, which is believed to be partly due to cleaner grain boundaries in the superconducting matrices.²⁰ For $\text{Cd} \geq 0.55$, the resistivity is increased, this enhancement of resistivity can be the result of whether from an interruption of intergrain contact. Therefore, the contact between superconducting phases weakens.

From the above results, it can be decided that the sample of $x = 0.35$ represents the optimum composition for obtaining nearly only 2212-phase in $\text{Bi}_{1.82}\text{Pb}_{0.36}\text{Sr}_2\text{Ca}_2\text{Cd}_x\text{Cu}_3\text{O}_y$ system. From the $(\rho-T)$ curve of the Cd-sample ($x = 0.35$) in Fig. 3, one can be noticed that the departure from the normal behaviour of resistivity around 102 K originates from thermal fluctuations of the superconducting order parameter as a result of which an excess conductivity appears. Aslamazov and Larkin (AL)²¹ studied this phenomenon and derived an expression for the excess conductivity as

$$\Delta\sigma = A\varepsilon^{-\lambda},$$

where A is a temperature independent parameter, ε is the reduced temperature and is expressed as follows:

$$\varepsilon = (T - T_c^{\text{mf}})/T_c^{\text{mf}},$$

T_c^{mf} being the mean-field critical temperature is given by the peak of ($d\rho/dT$ versus T) as shown in Fig. 4. The dimensional exponent, λ , is found from the slope of the $\text{Ln}(\Delta\sigma)$ versus $\text{Ln}(\varepsilon)$ as shown in Fig. 5. λ is -1.0 for 2D system is designated $\lambda_{2\text{D}}$ and -0.5 for 3D system is designated as $\lambda_{3\text{D}}$. The excess conductivity ($\Delta\sigma$) is evaluated from the resistivity curve in Fig. 3 using standard definition:

$$\Delta\sigma = \sigma_m - \sigma_n = 1/\rho_m - 1/\rho_n,$$

where ρ_m and ρ_n are the measured and normal resistivity of the sample respectively. The normal resistivity can be obtained by the extrapolation of the linear part of the $\rho(T)$ curve.

Figure 4 verifies the relation between $d\rho/dT$ and T , this relation gives one single peak at 98 K. This peak represents T_c^{mf} . For the composition $\text{Bi}_{1.82}\text{Pb}_{0.36}\text{Sr}_2\text{Ca}_2\text{Cd}_{0.35}\text{Cu}_3\text{O}_y$, the AL model was applied in Fig. 4.

Figure 5 shows the linear parts of the double logarithmic relations between $\Delta\sigma$ and the reduced temperature (ε). Each of these plots seemed consisting of two linear parts with two slopes, these slopes denote corresponding values for the critical exponent λ_1, λ_2 . Above $\text{Ln } \varepsilon = -0.9$, $\lambda_1 = -1.1$ which is close to the 2D value but very close to T_c^0 the slope changes to $\lambda_2 = -0.5$, which corresponds to the 3-dimensional value. This suggests that in the Bi-(2212) system a crossover from 2D to 3D occurs at delimiting temperature, this delimiting temperature is designated as the crossover temperature $T_0 \approx 137.8$ K. Lawrence and Doniach²² derived the excess conductivity due to thermodynamic fluctuations for a layered superconductor and the expression is

$$\Delta\sigma = (e^2/16\hbar d)\varepsilon^{-1/2}(\varepsilon + 4J)^{-1/2},$$

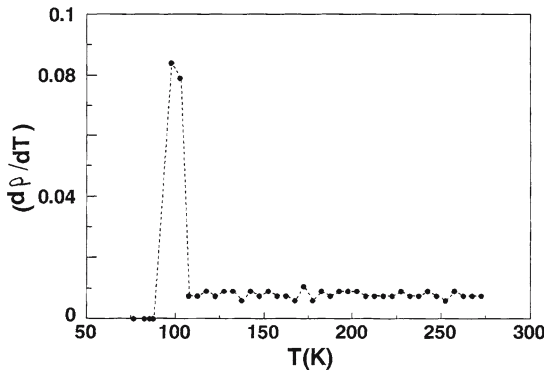


Fig. 4. Variation $d\rho/dT$ versus temperature of $\text{Bi}_{1.82}\text{Pb}_{0.36}\text{Sr}_2\text{Ca}_2\text{Cd}_{0.35}\text{Cu}_3\text{O}_y$.

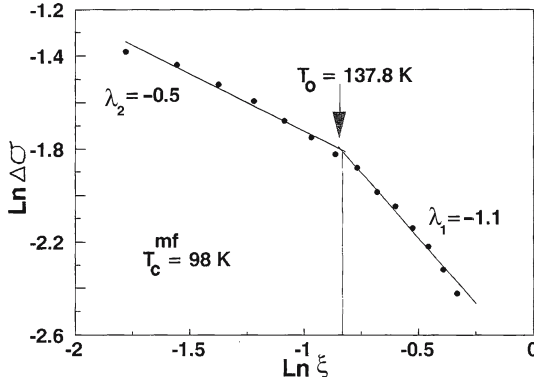


Fig. 5. The plot of $\text{Ln} \Delta\sigma$ versus $\text{Ln} \xi$ for $\text{Bi}_{1.82}\text{Pb}_{0.36}\text{Sr}_2\text{Ca}_2\text{Cd}_{0.35}\text{Cu}_3\text{O}_y$.

where $\varepsilon = (T - T_c^{\text{mf}})/T_c^{\text{mf}}$ is the reduced temperature, $J = [\xi(o)/d]^2$ is the inter layer coupling between superconducting layers. $\xi(o)$ represents the zero temperature coherence length and “ d ” is interlayer separation. The above expression suggests that there is a crossover from 2D to 3D behaviour as T_c^{mf} is approached. The crossover temperature T_0 is defined as²²

$$\varepsilon_0 = (T_0 - T_c^{\text{mf}})/T_c^{\text{mf}} = 4J.$$

In our system $T_0 = 137.8 \text{ K}$ and $T_c^{\text{mf}} = 98 \text{ K}$ which gives the interlayer coupling J as 10.1×10^{-2} comparing this value with that of Bi-2212 (5.5×10^{-3})²³ one finds that the interlayer coupling of Cd-sample ($x = 0.35$) is much harder than that for 2212 system.

3.4. SEM Observations

Figure 6(a–c) illustrates the surface morphology of compacts containing different contents of Cd in the system $\text{Bi}_{1.82}\text{Pb}_{0.36}\text{Sr}_2\text{Ca}_2\text{Cd}_x\text{Cu}_3\text{O}_y$ ($0.0 \leq x \leq 0.55$). As it is seen in Fig. 6(a), the free of Cd-sample shows the formation of light matrix which at first glimpse seems to be less regularly oriented. Šima et al.²⁴ reported that this matrix consists of both high and low superconducting phases. Another small white (bright) grains were also existed in close proximity to the light matrix. The colour of these grains is bright yellow or blue under polarized light.²⁵ This phase is similar in colour to the bronze phase, which was often observed in the undoped Bi–Sr–Ca–Cu–O system (thus, it is also known as the “bronze phase”).²⁵ Intercalation of 0.35 Cd resulted in Fig. 6(b), quite different microstructure which probably



Fig. 6. (a) Surface morphology of the powder compacts of the $\text{Bi}_{1.82}\text{Pb}_{0.36}\text{Sr}_2\text{Ca}_2\text{Cu}_3\text{O}_y$. Surface morphology of the powder compacts of the $\text{Bi}_{1.82}\text{Pb}_{0.36}\text{Sr}_2\text{Ca}_2\text{Cd}_{0.35}\text{Cu}_3\text{O}_y$. Surface morphology of the powder compacts of the $\text{Bi}_{1.82}\text{Pb}_{0.36}\text{Sr}_2\text{Ca}_2\text{Cd}_{0.55}\text{Cu}_3\text{O}_y$. (a–c) Surface morphology of the powder compacts of the $\text{Bi}_{1.82}\text{Pb}_{0.36}\text{Sr}_2\text{Ca}_2\text{Cd}_x\text{Cu}_3\text{O}_y$, (a) Cd ($x=0.0$), (b) Cd ($x=0.35$), (c) Cd ($x=0.55$).

depended on the compositional shift could be observed. Lamella (flake) shape grains become more abundant to appear with relatively large size. These flake grains are considered to be responsible for the low- T_c .²⁶ Also, these grains seem good link between them, well grain orientation and more homogeneous phase distribution in the matrix structure. This supports the contention that the addition of Cd up to 0.35 has the role of improvement of the surface morphology. Elevating the level of Cd to be 0.55 as shown in Fig. 6(c). As it is seen that the number and size of the flake grains slightly decreased with granular precipitations on mother grains, the link between the grains became weaker. Only small black lumps are dispersed in random way in the matrix. The black lumps probable to be corresponding to non-superconducting phases.²⁷

3.5. Microhardness and Porosity Measurements

Figure 7 shows variations of microhardness (VHN) with addition of Cd in the system of $\text{Bi}_{1.82}\text{Pb}_{0.36}\text{Sr}_2\text{Ca}_2\text{Cd}_x\text{Cu}_3\text{O}_y$ ($0.0 \leq x \leq 0.55$) at three considered loads (0.25, 0.49 and 0.98 N). It can be observed that at all the applied loads, an appreciable increase in VHN with enriching with Cd and it possessed maximum value at Cd ratio = 0.35. In contrast, values of VHN decreased slightly with more enriching with Cd to 0.55. This behaviour is probably due to the intercalation of cadmium between superconducting grains in compositions may provide a plastic-flow region that allows relaxation of undesirable stresses resulting from the grain anisot-

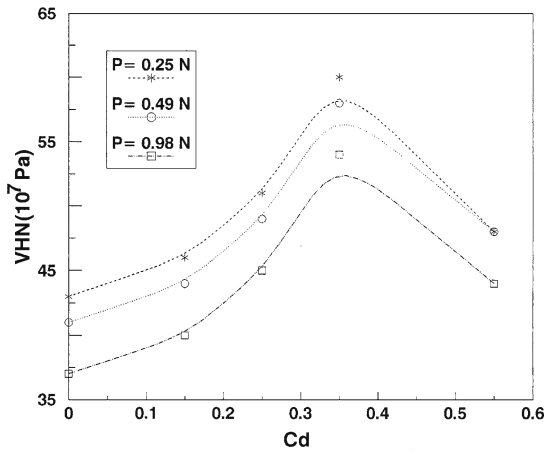


Fig. 7. The variation of microhardness with cadmium additions for $\text{Bi}_{1.82}\text{Pb}_{0.36}\text{Sr}_2\text{Ca}_2\text{Cd}_x\text{Cu}_3\text{O}_y$.

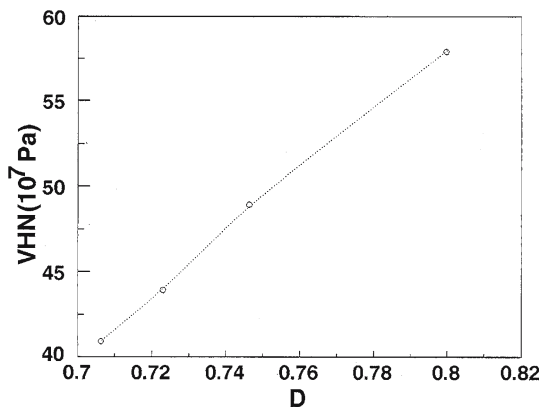


Fig. 8. The variation of microhardness with fractional density.

ropy of superconductors. Also, the presence of Cd may induce compressive stresses in the superconducting matrix due to the thermal expansion mismatch between superconductors and Cd particles. The compressive stresses in the superconducting matrix can be squeeze cracktips and impede crack propagation.

The variation of measured hardness (at 0.49 N load) with fractional density is shown in Fig. 8. The maximum hardness is 58×10^7 Pa for Cd-samples to 80% of theoretical density. The hardness varies approximately linearly with density. The measured hardness lies in the range reported by Khalil et al.²⁸ for BSCCO samples. Importantly, the hardness is an approximate indicator of the sample quality in that reduced porosity in the samples is clearly highly desirable. The close correlation between hardness and porosity offers a simple means of interrogating this quality by indirect means.

The effect of porosity on Young's modulus (E) is shown in Fig. 9, E was calculated at (0.49 N load). Fig. 9 seems that Young's modulus decreased exponentially as porosity increased. This trend could be explained by the presence of fine microcracks which do not alter the density significantly but which would have a deleterious effect on the mechanical parameters generally.

4. Conclusions

Structural formation, electrical property, excess conductivity and mechanical properties on the $\text{Bi}_{1.82}\text{Pb}_{0.36}\text{Sr}_2\text{Ca}_2\text{Cd}_x\text{Cu}_3\text{O}_y$ ($0.0 \leq x \leq 0.55$) have been studied. The following characteristics can be drawn based on the present experiments:

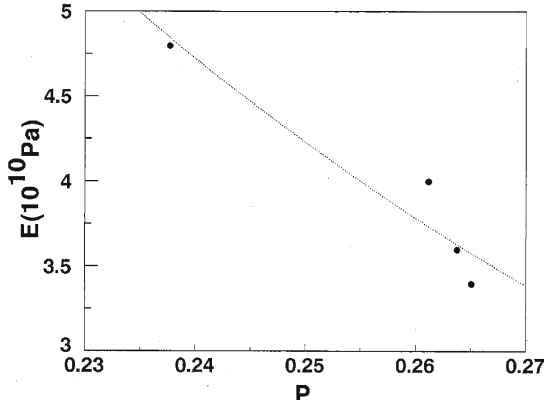


Fig. 9. The variation of Young's modulus with fraction porosity.

- 1 The XRPD pattern reveals that the 2223 phase and 2234 phase disappeared and the 2212 phase becomes dominant in Cd-doped sample of $x = 0.35$.
- 2 DTA results show a decrease in melting point of the samples with increase in Cd content.
- 3 $\rho - T$ characteristic indicates that an appropriate Cd addition of $x = 0.35$ makes the best superconducting properties.
- 4 A distinct 2D–3D crossover is observed in Cd-sample of $x = 0.35$ near T_c^0 from the excess conductivity analysis.
- 5 Interlayer coupling constant J is $\sim 10.1 \times 10^{-2}$ which greater than the value (5.5×10^{-3}) obtained for the 2212 system. This implies that the Cd-sample ($x = 0.35$) is more 2D in nature compared to the 2212 system.
- 6 SEM observations seem that the intercalation of Cd on the Bi-system has the role of improvement of the surface morphology in a way depends on its level in the compositions.
- 7 At Cd ($x = 0.35$) squeeze cracktips and impede crack propagation and hence resulting the best mechanical properties.

REFERENCES

1. S. M. Khalil, *J. Phys. Chem. solids* **62**, 457 (2001).
2. M. M. Ibrahim, S. M. Khalil, and A. M. Ahmed, *J. Phys. Chem. Solids* **61**, 1553 (2000).
3. N. Ichinose and A. Quema, *J. Magnet. Magnet. Mat.* **104**, 565 (1992).
4. K. Konstantinov and S. Karbanov, *Physica C* **165**, 170 (1990).
5. M. Yoshimura, T. Sung, N. Ishizawa, and Z. Nakagawa, *Jpn. J. Appl. Phys.* **28**, L424 (1989).

6. T. P. Beales, C. Dineen, W. G. Freeman, S. R. Hall, M. R. Harison, D. M. Jacobson, and S. J. Zammattio, *Supercond. Sci. Technol.* **5**, 47 (1992).
7. R. S. Liu, D. Groult, A. Maignan, S. F. Hu, D. A. Jefferson, B. Reveau, C. Michel, M. Hervieu, and P. P. Edwards, *Physica C* **195**, 35 (1992).
8. T. P. Beales, C. Dineen, S. R. Hall, M. K. Harrison, and J. M. Parberry, *Physica C* **207**, 1 (1993).
9. Q. Yitai, T. Kaibin, Y. Peidong, C. Zuyao, Li. Rukang, Z. Guien, Z. Yuheng, and W. Nanlin, *Physica C* **209**, 516 (1993).
10. P. de Villiers, R. A. Doyle, and V. V. Gridin, *J. Phys. Condens. Matter* **4**, 9401 (1992).
11. P. Mandal, A. Poddar, A. N. Das, B. Ghosh, and P. Choudhury, *Physica C* **169** 43 (1990).
12. S. M. Khalil, *J. Phys. Chem. solids* **64**, 855 (2003).
13. S. M. Khalil, *Smart Mater. Struct.* **14**, 804 (2005).
14. C. Veerender, V. R. Dumke, and M. Nagabhooshanam, *Phys. Stat. Sol. (a)* **144**, 299 (1994).
15. W. Xiaolin, W. Hong, S. Shuxia, W. Zhuo, and J. Minhua, *Solid State Commun.* **76**, 675 (1990).
16. T. Kaibin, Z. Yilei, C. Zuyao, Q. Yitai, C. Liezhao, and Z. Yuheng, *Physica C* **232**, 131 (1994).
17. S. Bernik, M. Hrovat, and D. Kolar, *Supercond. Sci. Technol.* **7**, 920 (1994).
18. T. Honda, T. Wada, M. Sakai, M. Miyanaga, N. Nishikawa, S. Uchida, K. Uchinokawa, and S. Tanaka, *Jpn. J. Appl. Phys.* **27**, L545 (1988).
19. S. X. Wang, Z. H. HE, X. H. Chen, M. R. Ji, Y. T. Qian, Z. Y. Chen, and Q. R. Zhang, *Phys. Stat. Sol. (a)* **115**, K71 (1989).
20. J. Joo, J. P. Singh, T. Warzynski, A. Grow, and R. B. Poeppel, *Appl. Supercond.* **2**, 401 (1994).
21. L. G. Aslamazov and A. I. Larkin, *Phys. Lett. A* **26**, 238 (1968).
22. W. E. Lawrence and S. Doniach, in *Proceeding of the Twelfth International Conference on Low Temperature Physics, Kyoto, Japan*, E. Kanda (ed.), Keigaku, Tokyo, (1971), p. 361.
23. P. Mandal, A. Poddar, A. N. Das, B. Ghosh, and P. Choudhury, *Physica C* **169**, 43 (1990).
24. V. Šima, K. Knizek, J. Chval, E. Pollert, P. Svoboda, and P. Vasek, *Physica C* **203**, 59 (1992).
25. C. J. Kim, C. K. Rhee, H. G. Lee, C. T. Lee, S. J-L. Kang, and D.Y. Won, *Jpn. J. Appl. Phys.* **28**, L45 (1989).
26. S. Adachi, O. Inoue, and S. Kawashima, *Jpn. J. Appl. Phys.* **27**, L344 (1988).
27. S. X. Dou, H. K. Liu, M. H. Apperley, K. H. Song, and C. C. Sorrell, *Physica C* **167**, 525 (1990).
28. S. M. Khalil and A. Sedky, *Physica B* **357**, 299 (2005).